Published in final edited form as:
*Circ Res*. 2011 April 15; 108(8): 908–916. doi:10.1161/CIRCRESAHA.110.239574.

# Echocardiographic Speckle-Tracking Based Strain Imaging for Rapid Cardiovascular Phenotyping in Mice

**Michael Bauer, MD**[1,*], **Susan Cheng, MD**[1,*], **Mohit Jain, MD, PhD**[1], **Soeun Ngoy**[1], **Catherine Theodoropoulos**[2], **Anna Trujillo**[2], **Fen-Chiung Lin, MD**[3], and **Ronglih Liao, PhD**[1]

[1]Cardiovascular Division, Department of Medicine, Brigham and Women's Hospital, Harvard Medical School, Boston, MA

[2]VisualSonics Inc, Toronto, Canada

[3]Cardiovascular Division, Chang Gung Memorial Hospital, Taipei, Taiwan

## Abstract

**Rationale—**High-sensitivity *in vivo* phenotyping of cardiac function is essential for evaluating genes of interest and novel therapies in small animal models of cardiovascular disease. Transthoracic echocardiography is the principal method currently used for assessing cardiac structure and function; however, standard echocardiographic techniques are relatively insensitive to early or subtle changes in cardiac performance, particularly in mice.

**Objective—**To develop and validate an echocardiographic strain imaging methodology for sensitive and rapid cardiac phenotyping in small animal models.

**Methods and Results—**Herein, we describe a modified echocardiographic technique that utilizes speckle-tracking based strain analysis for the non-invasive evaluation of cardiac performance in adult mice. This method is found to be rapid, reproducible, and highly sensitive in assessing both regional and global left ventricular (LV) function. Compared to conventional echocardiographic measures of LV structure and function, peak longitudinal strain and strain rate were able to detect changes in adult mouse hearts at an earlier time point following myocardial infarction (post-MI) and predicted the later development of adverse LV remodeling. Moreover, speckle-tracking based strain analysis was able to clearly identify subtle improvement in LV function that occurred early in response to standard post-MI cardiac therapy.

**Conclusions—**Our results highlight the utility of speckle-tracking based strain imaging for detecting discrete functional alterations in mouse models of cardiovascular disease in an efficient and comprehensive manner. Echocardiography speckle-tracking based strain analysis represents a method for relatively high-throughput and sensitive cardiac phenotyping, particularly in evaluating emerging cardiac agents and therapies in mice.

### Keywords

cardiac phenotyping; echocardiography; cardiac function; cardiovascular physiology; strain imaging

Correspondence: Ronglih Liao, PhD, Cardiac Muscle Research Laboratory, Cardiovascular Division, Department of Medicine, Brigham and Women's Hospital, Harvard Medical School, Phone:(617) 525-4854, Fax: (617) 525-4868, rliao@rics.bwh.harvard.edu.
[*]Denotes equal author contribution

**DISCLOSURES**

Catherine Theodoropoulosand Anna Trujillo are employees of VisualSonics. The remaining authors have no relevant disclosures.

## INTRODUCTION

The ability to assess cardiac performance in small animals is critically important for phenotyping genetic mouse models, evaluating the efficacy of novel cardiovascular disease therapies, and investigating the safety of agents with potential cardiotoxic side effects.[1, 2] Current approaches for assessing cardiac performance, however, are limited. *In vitro* assessment of cardiac cell function, while highly sensitive, is inadequate given the functional complexity of the cardiovascular system, which integrates global pump function, neurohormonal status, vascular properties, and systemic hemodynamics.[1] Conventional non-invasive *in vivo* methods of assessing cardiac performance allow for physiologic investigations but have limited resolution, which prevents capturing subtle alterations in cardiac function that can occur early in the course of myocardial injury or healing.[3, 4]

Despite the availability of multiple cardiac imaging modalities, a robust method for highly sensitive and rapid phenotyping of cardiac performance has yet to be established. Nuclear imaging techniques lack spatial resolution for performing detailed regional assessments, while cardiac magnetic resonance (CMR) and computed tomography techniques lack temporal resolution for characterizing discrete functional changes.[3–5] Furthermore, application of these imaging modalities in smaller animal models, especially mice, involves prohibitively expensive equipment, is time intensive, and may require complete procedural sedation that markedly alters *in vivo* hemodynamics. As a result, echocardiography has emerged in recent years as the standard cardiac imaging technique in experimental small animal models of cardiovascular disease.[6]

Echocardiography is non-invasive, widely available, cost-effective, and involves relatively short image acquisition and post-processing times.[3–6] Despite these advantages, conventional echocardiographic measures lack sensitivity for capturing subtle variations in left ventricular (LV) performance.[3, 4] Changes in LV structure and global function, when detected by conventional echocardiographic parameters, are typically considered late manifestations of disease.[7] Recently, a novel echocardiographic imaging technique, based on myocardial strain analysis, has been found to dramatically improve assessment of LV performance in humans.[8, 9] By capturing segmental tissue motion in multiple planes and axes serially over the cardiac cycle, strain analysis provides integrated and detailed information regarding both regional and global LV function – with much greater sensitivity and specificity than conventional echocardiographic measures, including fractional shortening (FS) or ejection fraction (EF).[8] To date, the adoption of strain imaging in small animal models has been limited, primarily due to technical differences in image acquisition and analysis in mice versus humans. However, recently developed speckle-tracking based techniques now allow for angle-independent, reproducible, and accurate strain measurements that may be applied to mice.

Herein, we describe a modified echocardiographic imaging methodology that utilizes speckle-tracking based strain analysis to conduct highly sensitive, non-invasive cardiac phenotyping in a mouse model of CV disease. Compared to conventional echocardiographic imaging, speckle-tracking based strain echocardiography was found to efficiently detect subtle changes in cardiac performance following myocardial infarction (MI) and also identify early differences in response to treatment with standard cardiac therapy. Thus, speckle-tracking based strain echocardiography represents a novel method for relatively high-throughput and sensitive cardiac phenotyping, including in the evaluation of emerging cardiac therapies in mouse models of cardiovascular disease.

# METHODS

An expanded Methods section is available in the Online Supplement and includes further detailed information regarding the experimental MI procedure, conventional echocardiographic measurements, *in vivo* speckle-tracking based strain echocardiography, pathologic cardiac assessment, and statistical analyses.

## Experimental Protocol

Adult C57BL/6J mice were obtained from Jackson Laboratory at 8 weeks of age, placed on a standard mouse chow diet and water ad libitum, and housed in a temperature-controlled environment under an alternating 12-hour light-dark cycle. All animal handling procedures adhered strictly to the approved guidelines of the Institutional Animal Care and Use Committee. A total of 16 mice (mean weight, 26.3±1.7 g) were randomly assigned to 1 of the following 3 groups: a group that underwent open thoractomy without coronary ligation ("sham", N=5); a group that underwent permanent left anterior descending artery (LAD) ligation without subsequent treatment ("MI", N=6); and, a group that underwent permanent LAD ligation followed by oral administration of an angiotensin converting enzyme inhibitor (ACEi) (captopril 20 mg/kg/day) in the drinking water starting on day 7 following surgery ("MI+ACEi", N=5). Coronary ligation was performed as previously described.[10] Echocardiography was performed on all mice under light sedation (1% isoflurane in oxygen) prior to surgery (baseline) and at 1 week following surgery (prior to starting any treatment with ACEi), at 3 weeks, and at 7 weeks following surgery. Echocardiography was performed using a 18–38 MHz linear-array transducer with a digital ultrasound system (Vevo 2100 Imaging System, VisualSonics, Toronto, Canada). Standard parasternal long- and short-axis views were obtained during each echocardiographic exam. Conventional and novel echocardiographic image measurements were performed offline. All image acquisitions and offline measurements included in the present analysis were conducted by a single investigator who was blinded to animal groups. At 7 weeks, mice were sacrificed for pathologic assessment of cardiac remodeling and infarct size.

## Conventional Echocardiographic Measurements

Echocardiographic measurements were obtained from grayscale M-mode images, at the mid-papillary level in the parasternal short-axis view, and also from B-mode images acquired in the parasternal long- and short-axis views. Conventional measurements of the LV included: end-diastolic diameter (LVEDD), end-systolic diameter, anterior and posterior wall thicknesses, fractional shortening (FS), wall thickening, fractional area change (FAC), end-systolic and end-diastolic volumes, ejection fraction (EF), and LV mass.

## Novel Echocardiographic Speckle-Tracking Based Strain Measures of Myocardial Deformation

Based on Lagrangian and Eulerian strain tensors of finite deformation theory, extensional *strain* of soft tissue in a pre-specified direction can be defined as the change in length of a segment divided by its original length ($[L_1-L_0]/L_0$), where *strain rate* (SR) is the rate of change of this deformation over time ($[(L_1-L_0)/L_0] \times \sec^{-1}$).[11] Using speckle-tracking based strain analysis of 2-dimensional gray-scale echocardiographic images acquired from the parasternal long- and short-axis views, strain and strain rate were quantified in the longitudinal, radial, and circumferential axes; in accordance with myocardial fiber orientation at varying levels of the LV wall, longitudinal strain is most representative of myocardial shortening at the level of the endocardium, while radial and circumferential strains are more reflective of shortening at the level of the mesocardium (Figure 1).

Parasternal long-axis views were found to provide the most reproducible myocardial views for longitudinal strain analyses in mice, whereas parasternal short-axis views (at the mid-papillary level) were obtained for circumferential and radial (short-axis) strain analyses (Figure 1A). All images were acquired at a frame rate of >200 frames/second (average 230 frames/second) and at an average depth of 11 mm.

Strain analyses were conducted by the same trained investigator on all animals according to the protocol detailed in the Online Supplement and using a speckle-tracking algorithm provided by VisualSonics (VevoStrain, VisualSonics). In brief, suitable B-mode loops were selected from digitally acquired echocardiographic images based on adequate visualization of the endocardial border and absence of image artifacts. Three consecutive cardiac cycles were selected for analysis based on image quality. Semi-automated tracing of the endocardial and epicardial borders were performed and verified over all 3 cardiac cycles, and then corrected as needed to achieve good quality tracking throughout each cine loop. Tracked images were then processed in a frame-by-frame manner for strain measurements (Figure 1B). Strain measures were averaged over the obtained cardiac cycles (with temporal smoothing filters turned off for all measurements), resulting in curvilinear strain and strain rate data (Figure 1C). Each long- and short-axis view of the LV myocardium was divided into 6 standard anatomic segments[12] for regional speckle-tracking based strain analysis throughout the cardiac cycle. In MI animals, the mid-anterior, apical-anterior, and apical-inferior wall segments were designated as the “infarct” region, and the basal-inferior and mid-inferior wall segments were designated as the “remote” (non-infarct) region. Peak strain and strain rate measurements were recorded from each of the 6 standard segments in each view, providing regional strain values. For global strain values, peak strain and strain rate measurements were averaged across all 6 segments. Regional strain values were obtained by averaging these same measurements across “infarct” and “remote” segments, respectively.

## RESULTS

### Echocardiographic Speckle-Tracking Based Strain Imaging

During each cardiac cycle, the LV undergoes a typical pattern of tissue deformation in multiple planes. This complex functional pattern includes myocardial shortening in the longitudinal axis, thickening in the radial axis, and shortening in the circumferential axis during systole – followed by reverse changes during diastole (Figure 1A). Myocardial tissue deformation in these axes can be assessed, both regionally and globally, as measures of tissue *strain* and *strain rate*. Speckle-tracking based strain analyses of myocardial motion (in the long-and short-axis images) integrates frame-to-frame data from cine loops (Figure 1B), allowing for measurements of segmental myocardial strain and calculation of strain rate in the longitudinal, radial, and circumferential axes. These measures are plotted as curvilinear data for each region tracked (Figure 1C).

Echocardiographic images were obtained in adult mice, as described in the Methods. Total time for image acquisition and analyses were similar for conventional and speckle-tracking based strain measures, and together totaled less than 25 minutes per animal, typically allowing for imaging and analysis of 20 mice per day by a single operator. Acquisition of B-mode images in the parasternal long-axis view, followed by acquisition of M-mode and B-mode images in the parasternal short-axis view, involved 2–5 minutes of image acquisition time per view. During image acquisition, mice were lightly anesthetized (1% isoflurane in oxygen). As demonstrated by average heart rates of 560±79 bpm at baseline (Table 1), echocardiography allowed for *in vivo* cardiac assessment at physiologic heart rates without significantly altering resting hemodynamics. All acquired images were deemed appropriate for both conventional and speckle-tracking based strain measurements.

Similar to conventional echocardiographic measures, speckle-tracking based strain analyses were performed offline after imaging acquisition was completed. Conventional and speckle-tracking based strain measurements involved a total of 7–15 minutes of analysis time per study (including image selection, image tracing/measuring, and data processing), where up to 15 minutes was needed for a minority of studies that required repeat image tracing and processing to avoid or minimize the effects of artifact on speckle-tracking. Speckle-tracking based strain measures exhibited high intra-observer and inter-observer reproducibility ($r=0.87$ and $r=0.89$, $P<0.001$ for both), comparable to recent human studies using similar methods.[13] Safety of the experimental procedure was demonstrated by lack of any adverse reactions or deaths observed for the animals studied over the duration of the study period.

## Novel Measures of Myocardial Performance Following Regional Myocardial Injury

To determine the relative sensitivity of speckle-tracking based strain measures versus conventional echocardiographic measures in the assessment of impaired cardiac function, adult mice were serially imaged following MI or sham operation. Both conventional and speckle-tracking based strain measures of myocardial performance were similar across all animals at baseline, prior to either MI or sham operation (Table 1).

**Global Function—**Within 1 week following MI or sham operation, conventional measures of remodeling (LVEDD and LV mass) increased and conventional measures of global LV function (FS and EF) decreased in MI compared to sham animals (Table 2, Figures 2A and 2B). Advanced measures of cardiac performance, represented by myocardial strain in all axes (longitudinal, radial, and circumferential), were also reduced early following MI (Table 3, Figures 2C and 2D) and these changes persisted over the total 7 week observation period (Table 3). These changes were most consistently significant for longitudinal compared to radial and circumferential strains, in accordance with greater vulnerability of endocardial and subendocardial tissue to ischemia from coronary obstruction. Importantly, changes in myocardial longitudinal strain and strain rate were more marked than changes in conventional LV measures, even FS (Figure 2E).

**Regional Function—**Strain analyses further allow for quantification of regional cardiac function within the infarct zone (mid-anterior, apical-anterior, and apical-inferior segments) and the remote, non-infarct zone (basal-inferior and mid-inferior segments). Interestingly, myocardial performance decreased at 1 week not only the infarct segments but also in regions remote from the designated infarct area (Table 3, Figure 2G), consistent with prior evaluations of regional myocardial function using CMR imaging in mice.[14] This pattern of regional dysfunction persisted over the total 7 week duration of follow up among animals in the MI group (Table 3).

## Ability of Myocardial Performance Measures to Differentiate Effects of MI Treatment

To determine the relative sensitivity of speckle-tracking based strain versus conventional measures in assessing the effects of potential cardiac therapies, a subset of the MI animals underwent treatment with ACEi (MI+ACEi) or served as vehicle control (MI). Serial echocardiography was performed before and after ACEi administration, which represents a mainstay of post-MI cardiac therapy and has been shown to improve both cardiac function and survival in animal models and humans.[15–17]

At serial time points following MI, progressive changes consistent with adverse ventricular remodeling were observed in all animals but, as expected, to a lesser degree in ACEi treated compared to untreated mice. Significant differences between MI and MI+ACEi mice in conventional structural measures, including LV chamber size and mass, were observed at 7 weeks following MI (6 weeks following treatment) (Table 2). However, conventional

measures of global cardiac function, such as FS and EF, failed to differentiate between MI and MI+ACEi vehicle mice within 3 weeks following MI (Figures 3A and 3B) or even over the total 6-week duration of follow up (Table 2). In contrast, advanced strain analysis of myocardial performance identified differences between ACEi and vehicle mice as early as 3 weeks following MI (2 weeks following treatment) (Table 3, Figures 3C and 3D). Even within this early follow-up period, global measures of peak longitudinal strain and strain rate were significantly better in ACEi compared to vehicle mice (Figures 3C and 3D). Interestingly, longitudinal strain assessed in the region remote from the infarct zone was also significantly greater in ACEi than in vehicle animals (Table 3). These differences suggest that improvement in myocardial function, as a result of ACEi therapy, occurs even in areas remote from the site of MI. Accordingly, longitudinal strain rate was higher across all wall segments in ACEi-treated compared to non-treated mice (Figure 3E).

### Relation of Early Myocardial Performance with Later Remodeling

To determine if early measures of myocardial strain are predictive of later ventricular remodeling, we examined the association of strain measures, assessed early following MI, with measures of adverse cardiac remodeling occurring later in the course of post-MI recovery. This analysis was focused on longitudinal strain measures given their known high sensitivity for identifying myocardial dysfunction following an acute injury.[18–20] Among all MI animals (n=11), these advanced measures of cardiac performance, assessed at 3 weeks following MI, were significantly associated with parameters of LV remodeling at 7 weeks. Both global longitudinal strain and strain rate at 3 weeks were strongly associated with 2D chamber dimension at 7 weeks, as represented by LVEDD (r=0.81 and r=0.82; P<0.01 for both). Similarly, global longitudinal strain and strain rate at 3 weeks were also strongly associated with subsequent hypertrophy at 7 weeks, as reflected by higher heart weight (r=0.76 and r=0.74; P<0.01 for both).

### Necropsy Assessment

Following echocardiography, post-mortem pathologic studies were performed at 7 weeks. In the sham, MI, and MI+ACEi groups, heart-to-body weight ratios were 6.46±0.27, 8.82±0.57, and 7.33±0.41, respectively. These weights were strongly correlated with echocardiographically assessed LV mass at 7 weeks (r=0.85; P<0.01). Histologic examination of infarct size was also performed on all animals. Echocardiographically determined infarct size at 7 weeks for the MI and MI+ACEi groups was 47±3% and 47±7%, respectively, whereas histological assessment of infarct size for the MI and MI+ACEi animals was 46±9% and 53±9%, respectively. For the total sample of MI animals, echocardiographic infarct size was strongly correlated to histologic infarct size (r=0.93; P<0.001).

## DISCUSSION

In this report, we describe the utility of a non-invasive imaging method for highly sensitive and rapid cardiac phenotyping in a small animal model of cardiovascular disease. Advanced speckle-tracking based strain measures of LV performance were not only more sensitive than conventional echocardiographic measures in detecting global changes in post-MI cardiac function, but they also allowed region-specific functional assessments in infarcted versus non-infarcted areas of myocardium. Furthermore, speckle-tracking based strain measures of myocardial performance differentiated response to standard cardiac therapy with an ACE inhibitor earlier than did conventional measures of either LV function or remodeling.

In clinical studies, subtle abnormalities in strain are associated with the presence of myopathic disease even in the setting of normal cardiac structure and function by conventional measures.[8] Moreover, cardiovascular risk factors result in impaired strain measures prior to the development of decreased LV EF or ventricular dilation.[8, 21] In experimental studies, the adoption of strain analysis to facilitate detailed cardiac phenotyping has been limited, primarily due to technical differences in imaging mice versus humans, including limited echocardiographic views, translational motion during image acquisition, and the effect of very high heart rates on the number of frames per second that may be captured and, in turn, analyzed. However, recently developed image analysis techniques, based on speckle-tracking, now allow for angle-independent and accurate strain-related measurements of mice at high frame rates.[22, 23] As such, recent studies have described the ability of speckle-tracking analyses to characterize serial changes in myocardial strain occurring in parallel with decrements in conventional measures of cardiac function in the setting of transverse aortic constriction[23, 24] and MI.[25] However, prior investigations have focused on speckle-tracking analyses of short-axis images, which precludes measures of longitudinal strain and, thus, limits the ability to assess the relative sensitivity of speckle-tracking versus conventional measures in mice.

Normal LV function involves a typical pattern of myocardial deformation that includes longitudinal shortening, circumferential shortening, and radial thickening in systole, followed by reverse changes in diastole.[26, 27] Reflecting myocardial fiber shortening at the level of the endocardium, alterations in longitudinal myocardial deformation tend to be among the earliest signs of cardiac dysfunction.[18–20] Compared to strain in the circumferential or radial axes, which predominantly reflect activity of the mesocardium (mid-myocardium), longitudinal strain is a particularly sensitive marker of the subendocardial myofiber dysfunction that tends to occur early in the setting of hypoperfusion or mechanical stress.[8, 28, 29] Accordingly, we observed that regional and global measures of longitudinal strain worsened dramatically and soon after experimental MI, which parallels findings from prior animal[25, 30, 31] and human[32–34] studies. In contrast to conventional echocardiographic measures, speckle-tracking based strain measures provided additional region-specific assessments of LV function, demonstrating impaired performance in non-infarcted as well as infarcted areas of the myocardium. Functional abnormalities affecting the myocardial tissue remote to the infarct region may be due to global myocardial stunning and hypoperfusion or continued ventricular remodeling.[30, 33] Using serial imaging, we observed that regional decrements in myocardial function appeared early in the course of recovery following MI and persisted throughout the study follow-up period, similar to prior studies using CMR in mice.[14] Further extending from CMR studies, which are predominantly limited to short-axis assessments of circumferential and radial strains,[35, 36] echocardiographic speckle-tracking in this study enabled evaluation of longitudinal strains and, thus, enhanced sensitivity for detecting early decrements in LV function following MI.

Our results also demonstrate that the serial application of speckle-tracking based strain measures is highly sensitive for identifying the beneficial effects of a pharmacologic therapy following MI. While conventional LV measures such as FS and LVEDD did not significantly differ between vehicle versus ACEi-treated mice until 7 weeks following MI, measures of longitudinal strain exhibited the benefit of standard therapy as early as 3 weeks following MI. Prior studies have shown that alterations in strain coincide with alterations in conventional measures of LV structure and function following MI,[25, 31, 32] likely due to the strong correlation between abnormal strain values and the extent of infarct.[25, 31, 34, 37, 38] Our data indicate that alterations in myocardial strain can both directly reflect evolving effects of a rescue therapy and also predict subsequent differences in LV remodeling. While the *long-term* benefits of ACE inhibitor therapy on preventing LV remodeling and

prolonging survival following MI have been long recognized,[15–17] our results highlight how the *early* ameliorative effects of ACE inhibitor therapy on myocardial performance can be observed even before differences in gross LV function or structure are detected. Furthermore, we demonstrate that strain abnormalities in both the infarcted and non-infarcted regions measurably improved in the setting of ACEi therapy. As with global strain, regional strain distinguished MI+ACEi from MI animals at an earlier time point than conventional measures of LV structure or function. The differential trajectories of myocardial response to MI, reflected by serial speckle-tracking based strain measures, may reflect the specific actions of ACEi on attenuating subendocardial hypoperfusion, hemodynamic load, and/or remodeling.[30, 39]

## Implications

We demonstrate the utility of a novel non-invasive imaging method for assessing cardiac function. Importantly, given the growing availability of genetically altered mice, this methodology may be used for rapid cardiovascular phenotyping in a relatively large number of animals. Furthermore, speckle-tracking based strain measures allow for rapid and sensitive assessment of cardiac function in response to either emerging therapies following injury or in response to potential cardiotoxic agents. This technique may be particularly useful when studying therapies such as cardiac regeneration, which may have specific regional, rather than global, effects.

## Study Limitations

Several limitations of this study merit consideration. Sources for variation exist in speckle-tracking based strain analysis, including the echocardiographic views obtained for image acquisition. Changes in the imaging angle of incidence can result in capturing different fiber layers at different levels and, thus, yield variable results. This is especially important for short-axis views where even small differences in image angle can lead to highly variable rotation and, in turn, circumferential strain measurements. Due to the presence of multiple orientation points (e.g. LV outflow tract, mitral valve leaflet plane, and LV apex), parasternal long axis views are less prone to angular variation in mice. Unlike in humans, apical 4-chamber views are difficult to obtain in mice and, therefore, parasternal long axis images are preferred for obtaining longitudinal strain measurements. Another source of variability is the tracing performed by the investigator, since strain values can depend on the quality and location of the tracing. As demonstrated by data from our laboratory, inter-observer variability can be minimized through use of a standardized detailed image analysis protocol.

Although segment-to-segment comparisons of LV strain measures are theoretically possible using speckle-tracking based strain analysis, discrimination of measurements at the single segment level is technically limited for serial evaluations in a post-MI model, in part due to the anatomic changes that result from remodeling. Notwithstanding this limitation, measures that are averaged across multiple segments, as employed in regional and global analyses, are both discriminating and reproducible. Speckle-tracking based analyses have also been used to evaluate post-MI dyssynchrony in humans;[40] however, these methods are not easily translated to mouse models, due largely to the much faster heart rates in mice. The applicability of the methods and generalizability of the findings reported herein may be limited to the use of similar equipment and software. However, continued advancements in the field of cardiac ultrasound are likely to broaden the availability of speckle-tracking based strain analyses, which rely on imaging systems that can accommodate high frame rates while preserving spatial as well as temporal resolution.

### Conclusion

In a small animal model, non-invasive echocardiographic assessment of myocardial deformation using speckle-tracking based strain analyses provided a highly sensitive *in vivo* characterization of distinct trajectories of LV dysfunction and remodeling following acute MI. Speckle-tracking based strain measures allowed for both detailed and efficient assessments of global and regional dysfunction which, in turn, predicted adverse remodeling. Thus, the use of speckle-tracking based strain measures to serially track regional and global myocardial performance parameters can provide insight into patterns of structural as well as functional myocardial recovery in response to cardiac therapies. This technique represents a novel approach to rapidly assessing phenotypic variation in the cardiac response to experimental myocardial injury and in the evaluation of therapies designed to attenuate the sequelae of such injury.

## Supplementary Material

Refer to Web version on PubMed Central for supplementary material.

## Acknowledgments

The authors wish to thank Mr. Frederic Roberts and Mr. Benjamin Deeley from VisualSonics for excellent technical support and helpful discussions, and Dr. Neal Lakdawala for insightful discussions.

**SOURCES OF FUNDING**

This work was supported in part by funding from the National Institutesof Health - HL088533, HL071775, HL093148, and HL099073 (RL). MB was a recipient of an American Heart Association founder affiliate postdoctoral fellowship award. SC was supported by an award from the Ellison Foundation and MJ was supported by NIH training grant T32HL007604.

## NON-STANDARD ABBREVIATIONS AND ACRONYMS

| | |
|---|---|
| **ACEi** | Angiotensin converting enzyme inhibitor |
| **CMR** | Cardiac magnetic resonance |
| **EF** | Ejection fraction |
| **FAC** | Fractional area change |
| **FS** | Fractional shortening |
| **LAD** | Left anterior descending (artery) |
| **LV** | Left ventricular |
| **LVEDD** | Left ventricular end-diastolic diameter |
| **LVWT** | Left ventricular wall thickness |
| **SR** | Strain rate |

## References

1. Christensen G, Wang Y, Chien KR. Physiological assessment of complex cardiac phenotypes in genetically engineered mice. Am J Physiol. 1997; 272:H2513–2524. [PubMed: 9227526]
2. Hanton G. Preclinical cardiac safety assessment of drugs. Drugs R D. 2007; 8:213–228. [PubMed: 17596108]
3. Marwick TH, Raman SV, Carrio I, Bax JJ. Recent developments in heart failure imaging. JACC Cardiovasc Imaging. 2010; 3:429–439. [PubMed: 20394905]

4. Stanton T, Marwick TH. Assessment of subendocardial structure and function. JACC Cardiovasc Imaging. 2010; 3:867–875. [PubMed: 20705269]
5. Lang RM, Bierig M, Devereux RB, Flachskampf FA, Foster E, Pellikka PA, Picard MH, Roman MJ, Seward J, Shanewise JS, Solomon SD, Spencer KT, Sutton MS, Stewart WJ. Recommendations for chamber quantification: a report from the American Society of Echocardiography's Guidelines and Standards Committee and the Chamber Quantification Writing Group, developed in conjunction with the European Association of Echocardiography, a branch of the European Society of Cardiology. J Am Soc Echocardiogr. 2005; 18:1440–1463. [PubMed: 16376782]
6. Hoit BD. Echocardiographic characterization of the cardiovascular phenotype in rodent models. Toxicol Pathol. 2006; 34:105–110. [PubMed: 16507551]
7. Borg AN, Ray SG. A unifying framework for understanding heart failure? J Am Soc Echocardiogr. 2009; 22:318–320. [PubMed: 19131209]
8. Cottrell C, Kirkpatrick JN. Echocardiographic strain imaging and its use in the clinical setting. Expert Rev Cardiovasc Ther. 2010; 8:93–102. [PubMed: 20030024]
9. Leitman M, Lysyansky P, Sidenko S, Shir V, Peleg E, Binenbaum M, Kaluski E, Krakover R, Vered Z. Two-dimensional strain-a novel software for real-time quantitative echocardiographic assessment of myocardial function. J Am Soc Echocardiogr. 2004; 17:1021–1029. [PubMed: 15452466]
10. Mouquet F, Pfister O, Jain M, Oikonomopoulos A, Ngoy S, Summer R, Fine A, Liao R. Restoration of cardiac progenitor cells after myocardial infarction by self-proliferation and selective homing of bone marrow-derived stem cells. Circ Res. 2005; 97:1090–1092. [PubMed: 16269652]
11. Heimdal A, Stoylen A, Torp H, Skjaerpe T. Real-time strain rate imaging of the left ventricle by ultrasound. J Am Soc Echocardiogr. 1998; 11:1013–1019. [PubMed: 9812093]
12. Cerqueira MD, Weissman NJ, Dilsizian V, Jacobs AK, Kaul S, Laskey WK, Pennell DJ, Rumberger JA, Ryan T, Verani MS. Standardized myocardial segmentation and nomenclature for tomographic imaging of the heart: a statement for healthcare professionals from the Cardiac Imaging Committee of the Council on Clinical Cardiology of the American Heart Association. Circulation. 2002; 105:539–542. [PubMed: 11815441]
13. Stanton T, Leano R, Marwick TH. Prediction of all-cause mortality from global longitudinal speckle strain: comparison with ejection fraction and wall motion scoring. Circ Cardiovasc Imaging. 2009; 2:356–364. [PubMed: 19808623]
14. Yang Z, Berr SS, Gilson WD, Toufektsian MC, French BA. Simultaneous evaluation of infarct size and cardiac function in intact mice by contrast-enhanced cardiac magnetic resonance imaging reveals contractile dysfunction in noninfarcted regions early after myocardial infarction. Circulation. 2004; 109:1161–1167. [PubMed: 14967719]
15. Pfeffer JM, Pfeffer MA, Braunwald E. Influence of chronic captopril therapy on the infarcted left ventricle of the rat. Circ Res. 1985; 57:84–95. [PubMed: 3891127]
16. Pfeffer MA, Braunwald E, Moye LA, Basta L, Brown EJ Jr, Cuddy TE, Davis BR, Geltman EM, Goldman S, Flaker GC, et al. Effect of captopril on mortality and morbidity in patients with left ventricular dysfunction after myocardial infarction. Results of the survival and ventricular enlargement trial. The SAVE Investigators. N Engl J Med. 1992; 327:669–677. [PubMed: 1386652]
17. Pfeffer MA, Pfeffer JM, Steinberg C, Finn P. Survival after an experimental myocardial infarction: beneficial effects of long-term therapy with captopril. Circulation. 1985; 72:406–412. [PubMed: 3891136]
18. Mizuguchi Y, Oishi Y, Miyoshi H, Iuchi A, Nagase N, Oki T. The functional role of longitudinal, circumferential, and radial myocardial deformation for regulating the early impairment of left ventricular contraction and relaxation in patients with cardiovascular risk factors: a study with two-dimensional strain imaging. J Am Soc Echocardiogr. 2008; 21:1138–1144. [PubMed: 18926389]
19. Wang J, Khoury DS, Yue Y, Torre-Amione G, Nagueh SF. Preserved left ventricular twist and circumferential deformation, but depressed longitudinal and radial deformation in patients with diastolic heart failure. Eur Heart J. 2008; 29:1283–1289. [PubMed: 18385117]

20. Zhang Q, Fung JW, Yip GW, Chan JY, Lee AP, Lam YY, Wu LW, Wu EB, Yu CM. Improvement of left ventricular myocardial short-axis, but not long-axis function or torsion after cardiac resynchronisation therapy: an assessment by two-dimensional speckle tracking. Heart. 2008; 94:1464–1471. [PubMed: 18198202]
21. Mondillo S, Galderisi M, Mele D, Cameli M, Lomoriello VS, Zaca V, Ballo P, D'Andrea A, Muraru D, Losi M, Agricola E, D'Errico A, Buralli S, Sciomer S, Nistri S, Badano L. Speckle-Tracking Echocardiography: A New Technique for Assessing Myocardial Function. J Ultrasound Med. 2011; 30:71–83. [PubMed: 21193707]
22. Leung DY, Ng AC. Emerging clinical role of strain imaging in echocardiography. Heart Lung Circ. 2010; 19:161–174. [PubMed: 20149727]
23. Peng Y, Popovic ZB, Sopko N, Drinko J, Zhang Z, Thomas JD, Penn MS. Speckle tracking echocardiography in the assessment of mouse models of cardiac dysfunction. Am J Physiol Heart Circ Physiol. 2009; 297:H811–820. [PubMed: 19561310]
24. Pistner A, Belmonte S, Coulthard T, Blaxall B. Murine echocardiography and ultrasound imaging. J Vis Exp. 2010:42.
25. Popovic ZB, Benejam C, Bian J, Mal N, Drinko J, Lee K, Forudi F, Reeg R, Greenberg NL, Thomas JD, Penn MS. Speckle-tracking echocardiography correctly identifies segmental left ventricular dysfunction induced by scarring in a rat model of myocardial infarction. Am J Physiol Heart Circ Physiol. 2007; 292:H2809–2816. [PubMed: 17277023]
26. Rosen BD, Gerber BL, Edvardsen T, Castillo E, Amado LC, Nasir K, Kraitchman DL, Osman NF, Bluemke DA, Lima JA. Late systolic onset of regional LV relaxation demonstrated in three-dimensional space by MRI tissue tagging. Am J Physiol Heart Circ Physiol. 2004; 287:H1740–1746. [PubMed: 15205167]
27. Sengupta PP, Krishnamoorthy VK, Korinek J, Narula J, Vannan MA, Lester SJ, Tajik JA, Seward JB, Khandheria BK, Belohlavek M. Left ventricular form and function revisited: applied translational science to cardiovascular ultrasound imaging. J Am Soc Echocardiogr. 2007; 20:539–551. [PubMed: 17485001]
28. Hashimoto I, Li X, Hejmadi Bhat A, Jones M, Zetts AD, Sahn DJ. Myocardial strain rate is a superior method for evaluation of left ventricular subendocardial function compared with tissue Doppler imaging. J Am Coll Cardiol. 2003; 42:1574–1583. [PubMed: 14607441]
29. Sabbah HN, Marzilli M, Stein PD. The relative role of subendocardium and subepicardium in left ventricular mechanics. Am J Physiol. 1981; 240:H920–926. [PubMed: 7246754]
30. Pislaru C, Bruce CJ, Anagnostopoulos PC, Allen JL, Seward JB, Pellikka PA, Ritman EL, Greenleaf JF. Ultrasound strain imaging of altered myocardial stiffness: stunned versus infarcted reperfused myocardium. Circulation. 2004; 109:2905–2910. [PubMed: 15173032]
31. Thibault H, Gomez L, Donal E, Augeul L, Scherrer-Crosbie M, Ovize M, Derumeaux G. Regional myocardial function after myocardial infarction in mice: a follow-up study by strain rate imaging. J Am Soc Echocardiogr. 2009; 22:198–205. [PubMed: 19121566]
32. Ingul CB, Malm S, Refsdal E, Hegbom K, Amundsen BH, Stoylen A. Recovery of function after acute myocardial infarction evaluated by tissue Doppler strain and strain rate. J Am Soc Echocardiogr. 2010; 23:432–438. [PubMed: 20202790]
33. Ingul CB, Stoylen A, Slordahl SA. Recovery of stunned myocardium in acute myocardial infarction quantified by strain rate imaging: a clinical study. J Am Soc Echocardiogr. 2005; 18:401–410. [PubMed: 15891749]
34. Zhang Y, Chan AK, Yu CM, Yip GW, Fung JW, Lam WW, So NM, Wang M, Wu EB, Wong JT, Sanderson JE. Strain rate imaging differentiates transmural from non-transmural myocardial infarction: a validation study using delayed-enhancement magnetic resonance imaging. J Am Coll Cardiol. 2005; 46:864–871. [PubMed: 16139138]
35. Gilson WD, Yang Z, French BA, Epstein FH. Measurement of myocardial mechanics in mice before and after infarction using multislice displacement-encoded MRI with 3D motion encoding. Am J Physiol Heart Circ Physiol. 2005; 288:H1491–1497. [PubMed: 15513963]
36. Li W, Yu X. Quantification of myocardial strain at early systole in mouse heart: restoration of undeformed tagging grid with single-point HARP. J Magn Reson Imaging. 2010; 32:608–614. [PubMed: 20815058]

37. Thibault H, Gomez L, Donal E, Pontier G, Scherrer-Crosbie M, Ovize M, Derumeaux G. Acute myocardial infarction in mice: assessment of transmurality by strain rate imaging. Am J Physiol Heart Circ Physiol. 2007; 293:H496–502. [PubMed: 17384134]

38. Weidemann F, Dommke C, Bijnens B, Claus P, D'Hooge J, Mertens P, Verbeken E, Maes A, Van de Werf F, De Scheerder I, Sutherland GR. Defining the transmurality of a chronic myocardial infarction by ultrasonic strain-rate imaging: implications for identifying intramural viability: an experimental study. Circulation. 2003; 107:883–888. [PubMed: 12591760]

39. Jones CJ, Raposo L, Gibson DG. Functional importance of the long axis dynamics of the human left ventricle. Br Heart J. 1990; 63:215–220. [PubMed: 2140044]

40. Shin SH, Hung CL, Uno H, Hassanein AH, Verma A, Bourgoun M, Kober L, Ghali JK, Velazquez EJ, Califf RM, Pfeffer MA, Solomon SD. Mechanical dyssynchrony after myocardial infarction in patients with left ventricular dysfunction, heart failure, or both. Circulation. 2010; 121:1096–1103. [PubMed: 20176989]

## Novelty and Significance

**What is Known?**

- Echocardiography (cardiac ultrasound) is frequently used to assess *in vivo* cardiac structure and function; however, conventional echocardiographic measures lack sensitivity for detecting changes early in the course of disease progression, particularly in commonly used small animal models of cardiovascular disease.
- A new echocardiographic method for high throughput and high sensitivity *in vivo* phenotyping of cardiac function is needed for evaluating genes of interest and novel therapies in small animal models of cardiovascular disease.

**What New Information Does This Article Contribute?**

- This article describes the novel application of echocardiographic strain imaging to mouse models of cardiovascular disease.
- In a mouse model of myocardial infarction (MI), echocardiographic strain-based measures allowed for assessment of global (whole heart) and regional (specific heart areas) cardiac function.
- Echocardiographic strain-based measures provided more sensitive and rapid assessment of cardiac structure and function in mice following MI and in response to cardiac therapy, relative to conventional echocardiographic measures.

Although transthoracic echocardiography is the principal method used for assessing cardiac structure and function, standard echocardiographic techniques are relatively insensitive to early or subtle changes in cardiac performance, particularly in mice. In this study, we describe a modified echocardiographic technique that utilizes speckle-tracking based strain analysis for the non-invasive evaluation of cardiac performance in adult mice. This method is rapid, reproducible, and highly sensitive in assessing regional and global LV function. Compared with conventional echocardiographic measures, peak longitudinal strain and strain rate were able to detect changes in adult mouse hearts at an earlier time point following MI and predicted the later development of adverse LV remodeling. Moreover, speckle-tracking based strain analysis was able to identify subtle improvement in LV function that occurred early in response to standard post-MI cardiac therapy. These results highlight the utility of speckle-tracking based strain imaging for detecting discrete functional alterations in mouse models of cardiovascular disease in an efficient and comprehensive manner. Thus, echocardiographic speckle-tracking based strain analysis represents a method for relatively high-throughput and sensitive cardiac phenotyping and evaluating potential therapies, in mice.

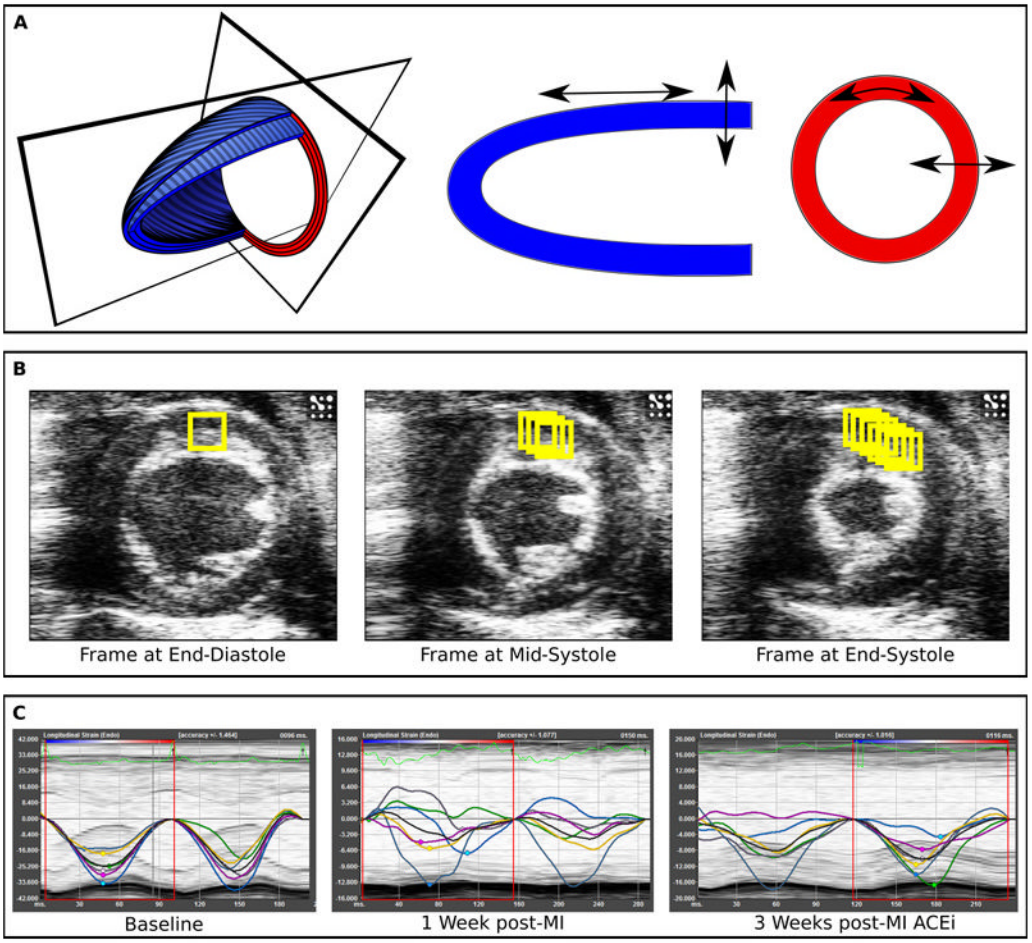


**Figure 1. Speckle-tracking based strain analysis**

Normal ventricular function involves myocardial deformation along the longitudinal, radial, and circumferential axes (Panel A). Speckle-tracking based strain analysis uses acoustic back scatter on echocardiographic images as tissue markers, which are tracked frame-to-frame throughout the cardiac cycle (Panel B). Timed tracking of myocardial deformation allows for the direct measurement of myocardial *strain* in the longitudinal, circumferential, and radial axes. For each axis, separate strain curves (representing strain measures over time) are generated for each of the six standard myocardial regions, with a $7^{th}$ line (black) denoting the average (global) strain at each time point (Panel C). Regional and global strain curves are altered in a typical fashion following MI and with ACEi treatment.

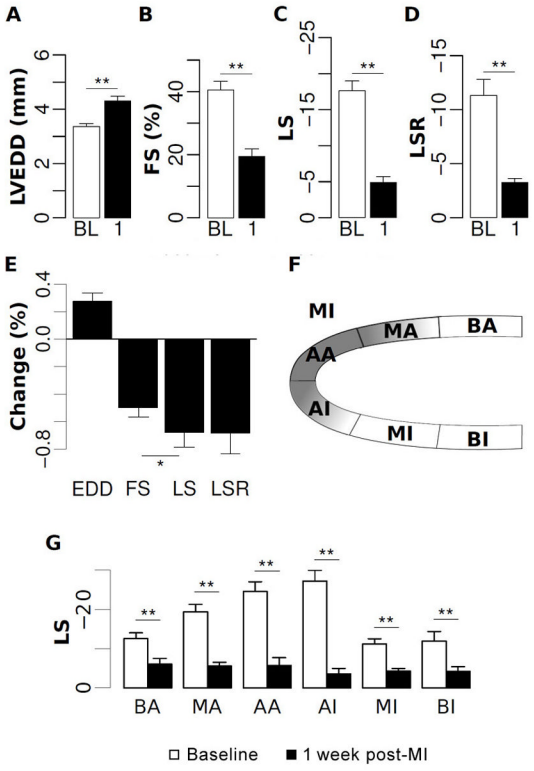


**Figure 2. Echocardiographic assessment of post-MI LV function and remodeling**

Among animals that underwent MI, changes in echocardiographic measures are shown at baseline (BL) and at 1 week post-MI (1). LV end-diastolic dimension (Panel A) was increased post-MI, whereas fractional shortening (Panel B), global peak longitudinal strain (Panel C), and global peak longitudinal strain rate (Panel D) all decreased with cardiac injury. Percent change in strain measures was greater than for conventional measures (Panel E). A schematic of myocardial regions identified from the parasternal long axis view is shown in Panel F: BA, basal anterior; MA, mid anterior; AA, apical anterior; AI, apical inferior; MI, mid inferior; BI, basal inferior. Peak longitudinal strain across these regions was normally distributed at baseline but globally reduced at 1 week post-MI (Panel G). *=$p<0.05$; **=$p<0.01$.

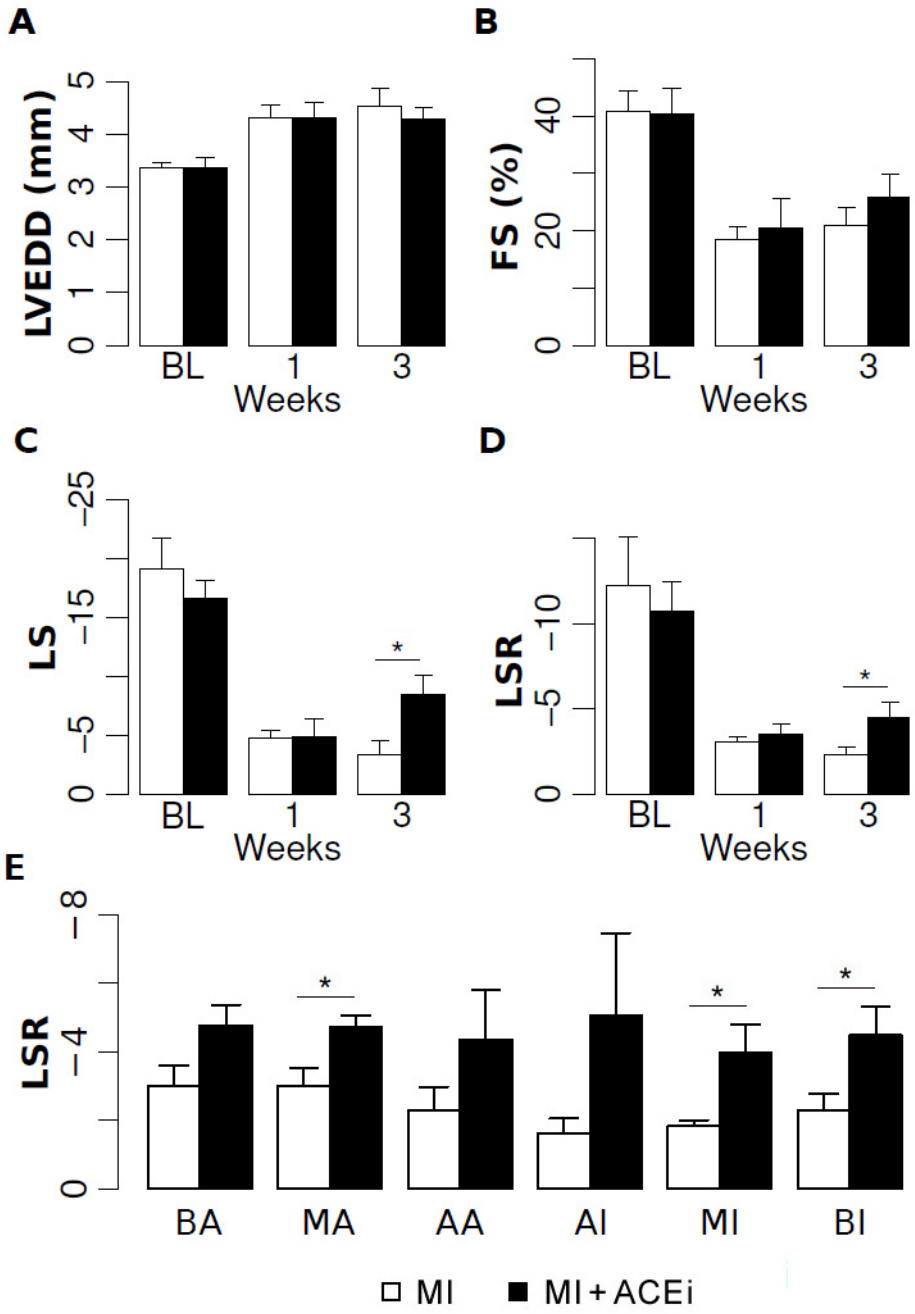


**Figure 3. Longitudinal changes in LV function and remodeling post-MI with cardiac therapy**

Echocardiographic measures are shown at baseline and at 1 week and at 3 weeks post-MI, for animals treated with vehicle (open bars) or ACE inhibition (filled bars). Conventional echocardiographic measures, including LVEDD (Panel A) and FS (Panel B) were unchanged in the early post-MI period with ACEi treatment, whereas both longitudinal strain (Panel C) and strain rate (Panel D) were significantly higher in ACEi treated versus untreated animals at 3 weeks. At 3 weeks, longitudinal strain rate was improved not only globally, but also across all segmental myocardial regions in ACEi treated compared to untreated animals (Panel E). Abbreviations for myocardial regions used in Panel E are previously defined in Figure 2, Panel F. *=$p<0.05$.

**Table 1**

Baseline Echocardiographic Characteristics

| | Sham | MI | MI + ACEi |
|---|---|---|---|
| **Conventional Measures** | | | |
| Heart rate, bpm | 513±32 | 584±45 | 520±26 |
| LVWT, mm | 0.8±0 | 0.8±0.1 | 0.8±0.1 |
| LVEDD, mm | 3.2±0.2 | 3.4±0.1 | 3.4±0.2 |
| FS, % | 38.6±3.8 | 40.8±3.5 | 40.3±4.6 |
| LV area long axis *, $mm^2$ | 20.5±1.1 | 16.0±1.4 | 16.4±0.8 |
| FAC long axis, % | 30.6±2.1 | 42.3±3.8 | 41.6±6.9 |
| LV area short axis *, $mm^2$ | 10.0±0.7 | 9.4±0.8 | 7.4±0.1 |
| FAC short axis, % | 48.7±3.3 | 56.6±5.4 | 61.4±4.8 |
| EF, % | 45.2±3.2 | 59.2±4.7 | 56.5±8.1 |
| LV mass, mg | 169.4±14.8 | 140.4±6.3 | 127.3±11.4 |
| **Strain Measures** | | | |
| ***Short Axis, %*** | | | |
| Circumferential strain | −28.7±2.5 | −31.1±3.1 | −30.1±3.8 |
| Circumferential SR | −12.2±2.4 | −13.4±2.4 | −13.0±1.9 |
| Radial strain | 31.6±3.8 | 39.0±2.4 | 34.9±4.8 |
| Radial SR | 8.9±1.2 | 11.3±0.9 | 10.8±1.1 |
| ***Long Axis, %*** | | | |
| Longitudinal strain | −17.9±1.5 | −19.1±2.7 | −16.6±1.5 |
| Longitudinal SR | −10.6±1.4 | −12.2±2.8 | −10.7±1.7 |
| Radial strain | 22.6±4.3 | 24.8±2.0 | 23.0±2.9 |
| Radial SR | 8.0±1.4 | 8.5±0.5 | 7.4±0.6 |

Values are shown as mean±SE.

* Measured at end-diastole.

*Circ Res*. Author manuscript; available in PMC 2012 June 18.

**Table 2**

Conventional Echocardiographic Measurements Over the Treatment Period

| | 1 week | | | 3 weeks | | | 7 weeks | | |
|---|---|---|---|---|---|---|---|---|---|
| | **Sham** | **MI** | **MI+ACEi** | **Sham** | **MI** | **MI+ACEi** | **Sham** | **MI** | **MI+ACEi** |
| LVWT, mm | 0.8±0 | 1.0±0.1 | 0.8±0.1 | 0.9±0.1 | 1.1±0.1 | 0.9±0.1 | 0.9±0 | 1.1±0.2 | 1.0±0.2 |
| LVEDD, mm | 3.1±0.2 | 4.3±0.2† | 4.4±0.2† | 3.0±0.2 | 4.5±0.3† | 4.3±0.2† | 3.1±0.1 | 5.1±0.4† | 4.2±0.5 |
| FS, % | 35.1±5.2 | 18.6±2.1† | 19.9±4.2† | 41.7±4.3 | 20.9±3.2† | 25.9±3.9† | 37.7±3.9 | 18.7±2.3† | 22.5±3.6† |
| LV area long axis‡, mm² | 16.0±1.6 | 30.2±3.3† | 27.9±2.1† | 16.2±0.7 | 34.0±3.3† | 26.6±2.7† | 17.7±1.4 | 37.9±5.5† | 28.6±2.5 |
| FAC long axis, % | 43.7±2.6 | 16.3±4.5† | 17.9±5.6† | 46.5±3.1 | 15.6±3.0† | 21.8±5.0† | 35.8±4.0 | 12.9±3.1 | 19.3±5.3† |
| LV area short axis‡, mm² | 8.0±0.7 | 16.4±2.1† | 15.9±1.6† | 8.2±0.8 | 18.9±2.2† | 14.6±0.9† | 8.4±0.5 | 21.4±2.5† | 13.8±1.5* |
| FAC short axis, % | 52.3±4.9 | 25.4±3.9† | 27.0±4.2† | 55.6±2.3 | 25.4±4.1† | 38.0±5.8† | 47.9±3.4 | 28.1±2.2† | 30.4±2.9† |
| EF, % | 60.5±3.4 | 23.4±7.0† | 25.3±7.3† | 63.6±3.9 | 23.4±4.6† | 33.2±6.8† | 50.8±4.8 | 20.7±4.9† | 29.5±7.0† |
| LV mass, mg | 129.6±4.8 | 186.5±12.2† | 186.1±8.9† | 145.7±9.4 | 166.9±5.4 | 151.5±6.4 | 142.4±10.4 | 202.3±18.3† | 140.8±8.4* |

Values are shown as mean±SE.

*p<0.05 vs. MI

†p<0.05 vs. Sham

‡Measured at end-diastole.

**Table 3**

Speckle-Tracking Based Strain Measurements Over the Treatment Period

| | 1 week | | | 3 weeks | | | 7 weeks | | |
|---|---|---|---|---|---|---|---|---|---|
| | **Sham** | **MI** | **MI+ACEi** | **Sham** | **MI** | **MI+ACEi** | **Sham** | **MI** | **MI+ACEi** |
| **Global, %** | | | | | | | | | |
| ***Short Axis*** | | | | | | | | | |
| Circum. strain | −25.9±2.7 | −13.9±0.8† | −10.7±1.6† | −27.7±3.1 | −12.9±1.2† | −19.0±3.9 | −25.9±3.2 | −12.5±1† | −12.7±1.1† |
| Circum. SR | −13.2±1.4 | −5.5±0.5† | −5.2±0.8† | −14.0±2.1 | −6.1±0.7† | −9.4±1.8 | −11.7±1.8 | −4.7±0.5† | −6.6±1.0† |
| Radial strain | 32.2±2.4 | 15.6±2.9† | 13.0±2.7† | 28.4±3.9 | 17.1±2.5 | 24.2±4.6 | 32.5±3.9 | 20.9±2.0† | 22.4±1.2† |
| Radial SR | 10.7±0.8 | 6.0±0.4† | 6.1±0.5† | 9.5±1.4 | 6.6±0.6 | 9.6±0.5 | 9.9±1.3 | 6.5±0.4† | 7.5±0.3 |
| ***Long Axis*** | | | | | | | | | |
| Long. strain | −15.7±1.5 | −4.9±0.6† | −4.9±1.6† | −15.3±1.2 | −3.4±1.2† | −8.6±1.6*† | −15.4±2 | −3.9±1.2† | −7.4±1.7† |
| Long. SR | −7.4±0.6 | −3.0±0.3† | −3.5±0.6† | −7.4±0.6 | −2.3±0.4† | −4.5±0.9*† | −7.1±1.1 | −2.9±0.6† | −4.1±0.8 |
| Radial strain | 19.4±2.5 | 9.9±1.9† | 12.6±2.2 | 19.6±3.1 | 8.0±1.3† | 11.7±3.9 | 19.9±3.2 | 7.5±1.6† | 13.2±3.2 |
| Radial SR | 8.0±0.7 | 5.9±1.0 | 7.8±0.6 | 7.7±0.9 | 5.2±0.1 | 7.8±1.1 | 7.4±1.2 | 6.7±0.7 | 8.0±0.7 |
| **Infarct Region, %** | | | | | | | | | |
| ***Long Axis*** | | | | | | | | | |
| Long. strain | −20.5±2.1 | −3.9±0.7† | −6.0±2.6† | −20.1±2.0 | −2.7±1.3† | −8.4±2.6† | −19.8±3.0 | −4.0±1.3† | −8.7±3.6† |
| Long. SR | −9.5±1.1 | −2.9±0.5† | −4.1±1.0† | −9.0±1.1 | −2.3±0.5† | −4.7±1.4† | −8.8±1.7 | −2.9±0.5† | −4.5±1.5 |
| Radial strain | 18.8±3.4 | 9.2±1.2† | 13.2±2.5 | 19.3±3.7 | 6.8±1.5† | 11.2±4.1 | 20.9±4.5 | 6.1±1.5† | 14.7±4.4 |
| Radial SR | 21.7±2.1 | 10.4±3.5† | 9.6±2.1† | 24.4±5.0 | 7.9±3.1† | 10.2±3.8 | 23.8±3.2 | 7.1±2.2† | 11.2±3.1† |
| **Remote Region, %** | | | | | | | | | |
| ***Long Axis*** | | | | | | | | | |
| Long. strain | −11.0±1.0 | −5.6±1.2† | −2.9±0.6† | −11.9±1.2 | −3.5±1.0† | −8.3±1.6* | −12.2±1.5 | −2.8±1.3† | −7.3±1.4 |
| Long. SR | −5.1±0.6 | −3.3±0.4† | −2.6±0.3† | −6.5±0.9 | −2.1±0.3† | −4.2±0.7 | −5.9±1.1 | −2.9±0.8 | −4.3±0.5 |
| Radial strain | 7.6±0.7 | 6.8±1.6 | 8.7±0.4 | 8.1±1.3 | 5.6±0.4 | 8.5±1.3 | 7.4±1.5 | 7.5±0.8 | 9.5±0.9 |
| Radial SR | 8.5±1.1 | 4.9±0.7 | 6.6±1.2 | 7.6±0.9 | 4.5±0.5† | 7.1±0.9 | 7.4±1.0 | 6.0±0.5 | 6.8±0.7 |

Values are shown as mean±SE.

* $p<0.05$ vs. MI

† $p<0.05$ vs. Sham